Scanning probe microscopy

DOI: 10.1002/smll.200700580

# Constrained Molecular Manipulation Mediated by Attractive and Repulsive Tip–Adsorbate Forces**

*Natalia Martsinovich, Lev Kantorovich, Richard H. J. Fawcett, Martin J. Humphry, and Peter H. Beton**

The forces between the tip of a scanning tunneling microscope and an adsorbed molecule may be exploited to induce a range of translational and conformational modes of manipulation.[1–12] As shown by Bartels et. al.,[2] different modes of translational manipulation may be distinguished through the acquisition of the trajectory executed by the scanning tunneling microscopy (STM) instrument tip as the adsorbate moves across the surface. In most cases the tip height changes abruptly as the molecule is translated between discrete adsorption sites on the surface, enabling a distinction between attractive and repulsive modes of manipulation. The abrupt change occurs when the molecule hops, since there is an effective change in the tip–surface separation, which results, when operating under constant-current mode, in an adjustment of tip height. An interesting variant, which occurs for weakly bound adsorbates under low-temperature conditions, is a sliding mode, in which discontinuous changes in tip height are absent and the adsorbate moves across the surface in a quasi-continuous manner rather than hopping between discrete adsorption sites.[2] In this Communication, we describe a mode of manipulation in which a balance between attractive and repulsive tip–molecule forces results in the stabilization of a molecule at a series of intermediate positions between the adsorption sites adopted by a free molecule on the surface. We find that the tip induces a type of repulsive manipulation, in which abrupt molecular hops are suppressed through a residual attractive interaction with the tip. There are some similarities between the acquired STM line scans and those previously categorized as sliding in low-temperature experiments.[2] However, for the large, strongly bound, molecule considered here, the motion differs significantly from a sliding trajectory.

[*] Dr. N. Martsinovich, Dr. L. Kantorovich
Department of Physics, Kings College London
London, WC2R 2LS (UK)

Dr. R. H. J. Fawcett, Dr. M. J. Humphry, Prof. P. H. Beton
School of Physics and Astronomy, University of Nottingham
Nottingham NG7 2RD (UK)
Fax: (+44) 115-951-5187
E-mail: peter.beton@nottingham.ac.uk

[**] We would like to acknowledge the computer time on the HPCx supercomputer via the Materials Chemistry Consortium and the financial support from the NANOMAN (NMP-CT-2003-505660) project and the Engineering and Physical Sciences Research Council (Grant EP/C534158/1).

Our investigations are performed using $C_{60}$ adsorbed on Si(100)-2 × 1 (see Experimental Section), which provides a model system for combined experimental and theoretical studies of the manipulation of covalently bound molecules.[13–17] An STM image, and schematic, of a single $C_{60}$ molecule on the Si(100)-2 × 1 surface is shown in the inset of Figure 1. The molecule is adsorbed in a 'trough' site midway between the dimer rows, which form on this surface.[18–20] Manipulation was performed both parallel and perpendicular to the dimer rows, while recording the tip trajectory as described in the Experimental Section.

Typical tip trajectories are shown in Figure 1. All traces show a complex waveform with a lateral periodicity of $na_0$, where $a_0$ (3.84 Å) is the lattice constant of the Si(100) surface and $n = 2$, 3, or 4. We have shown[16,17] that for manipulation along the trough (parallel to the dimer row) this long-range periodicity is due to molecular rolling. The large observed periodicity arises from the sequential bonding of the fullerene in different orientations during the rolling process. Fullerene rolling on this surface was proposed in the literature[13] and has also been discussed in the context of other surfaces.[9,21,22]

In Figure 1a–d we show line scans for molecules manipulated parallel (a and b) and perpendicular (c and d) to the dimer rows. While these periodic traces are a signature of repulsive molecular rolling along the troughs or across the rows, the curves also illustrate a feature of great significance, which we attribute to a combined attractive and repulsive tip–molecule interaction. In particular, we observe a gradient of the tip trajectory after molecular manipulation commences, which is much smaller than that expected if the molecule simply hops directly to a neighboring adsorption site. An example is shown in Figure 1a and is marked by the arrow A. To highlight the difference with previously observed traces, arrow B on the same trace identifies a much steeper tip-height change (with a gradient that is instrumentally limited) as expected for a molecule that abruptly hops to a neighboring adsorption site.

The other curves in Figure 1 provide further examples of line scans with finite gradients following the initiation of manipulation. Figure 1b shows an example of parallel manipulation with a different periodicity of $2a_0$ and small gradients. Figure 1c and d shows line scans for manipulation across a row. Figure 1c may be interpreted as follows: the molecule is displaced from a trough site to an adsorption site on top of the row (this corresponds to the step that occurs at a tip position of ca. 13 Å). A further displacement then results in the molecule being moved to a site in the neighboring trough (tip position of ca. 16 Å). The cycle is then repeated, giving rise to the trace with periodicity $2a_0$, in which successive steps correspond alternately to row–trough and trough–row transitions. The temporary stabilization of the molecule on top of the dimer row is of interest as molecules are not normally adsorbed on this site. Chen et al.[20] report approximately 5% of molecules on top of rows, although at this level it is possible that this is due to the presence of defects. Figure 1d shows a line scan for manipulation across a row in which the temporary stabilization on a row site is not effective.

For both parallel and perpendicular traces we observe sections with a range of 0.5–2.0 Å, over which the tip stabilizes

  

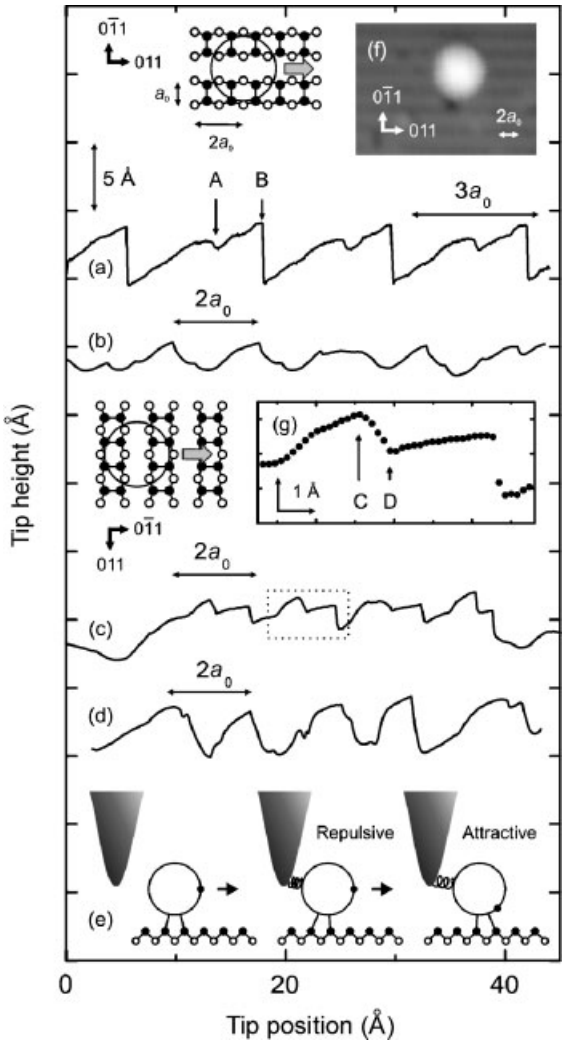


**Figure 1.** Tip trajectories for manipulation a,b) parallel and c,d) perpendicular to dimer rows. Sample voltage and tunnel current for these traces were: a) −0.3 V, 0.4 nA; b) −1 V, 1.65 nA; c) −1.3 V, 2.2 nA; d) −1.3 V, 2.2 nA. e) Schematic of tip–molecule interaction. f) STM image of adsorbed $C_{60}$ on Si(100)-2 × 1. g) Detail of highlighted segment of curve (c). Also shown are schematics of surface with directions of manipulation. The full circles represent top-layer silicon atoms, while the open circles represent second-layer silicon atoms.

the molecule at several intermediate points between neighboring adsorption sites. This is highlighted in Figure 1g, which shows a higher resolution plot for the highlighted part of curve Figure 1c: one can see several intermediate stable points between the maximum and minimum marked by arrows C and D, respectively. The observation that the molecule may be stabilized at intermediate positions between the adsorption sites on the surface is of critical importance. Specifically this observation implies that the combination of forces between a molecule, the STM tip, and the surface results in a series of new positions where a stable equilibrium occurs. As the tip is moved laterally across the surface, the position of this equilibrium shifts but at each point the attractive force between the tip and molecule is sufficiently strong to suppress an abrupt hop of the molecule to the neighboring trough site. Thus, the molecule is 'stuck' to both the tip and the surface. A simple schematic that shows the balance of these forces is shown in Figure 1e.

The central hypothesis of our explanation is that the attractive tip–molecule forces can overcome the tendency of the $C_{60}$ molecule to hop directly to a neighboring adsorption site. To determine whether this hypothesis is valid we have used density functional theory to calculate the interaction between a variety of model tip geometries and a fullerene molecule. We note that the geometry and composition of the tip used in the actual experiment is not known since tips are readily contaminated with the surface atoms during experiments;[23,24] however, a silicon tip would represent a reasonable model in our case. We have checked (numerically) that Si atoms readily bind to a tungsten cluster, with a binding energy of around 3.5 eV. Note also that recent theoretical simulations[25] of STM images of the Si(111) surface with silicon tips reproduced experimental images better than simulations done using tungsten tips, thus, suggesting that metallic tips in experiments are terminated by silicon. Therefore, our silicon tips are a valid model for describing the behavior of the tips used in the STM experiments. We present results for a particular tip geometry formed from a (111)-oriented, atomically sharp silicon tip terminated by a single dangling bond at its apex and with all other dangling bonds passivated through the addition of hydrogens. In our tip, the apex Si atom is bonded to three other Si atoms; thus, representing a stable Si cluster. The cluster we use is a reasonable compromise between the computational feasibility and realistic description of the system.[23,24,26] Moreover our objective is not to directly simulate the detailed atomic structure of a tip, which is not a realistic goal, but rather to determine whether any tip could lead to the stabilizing effect that we attribute to tip–molecule bonding. We have also considered alternative tip models (see below).

In our calculations (see Experimental Section), the $C_{60}$ molecule was initially positioned in the lowest-energy configuration (classified as *t*4*c* in Ref. [27]). The tip was positioned such that its apex atom was 5 Å from the center of the $C_{60}$ molecule and 8 Å above the surface (approximately level with the top of the $C_{60}$). The tip is displaced parallel to the trough in steps of 0.05 Å towards the molecule at a fixed height, and all atoms (except for the upper tip atoms and the lower 2 layers of the slab modelling the surface) were fully relaxed after each tip displacement.

The total energy of the combined tip–molecule–surface system is plotted as a function of tip position in Figure 2a. The energy reference is the total energy of the isolated $C_{60}$, STM tip, and the p-(2 × 1) reconstructed Si(001) surface, and is further corrected to take account of the basis set superposition error (BSSE).[28] In Figure 2b the *x*, *y*, and *z* coordinates (defined in the inset of Figure 2b) of the center of mass of the molecule as a function of tip position are plotted.

Figure 2a clearly shows that the overall energy rises rapidly as the tip is moved towards the molecule. This is followed by a number of abrupt reductions (marked by arrows A–E) in energy due to molecular re-bonding. These are accompanied by abrupt, but small, changes in the molecular

  

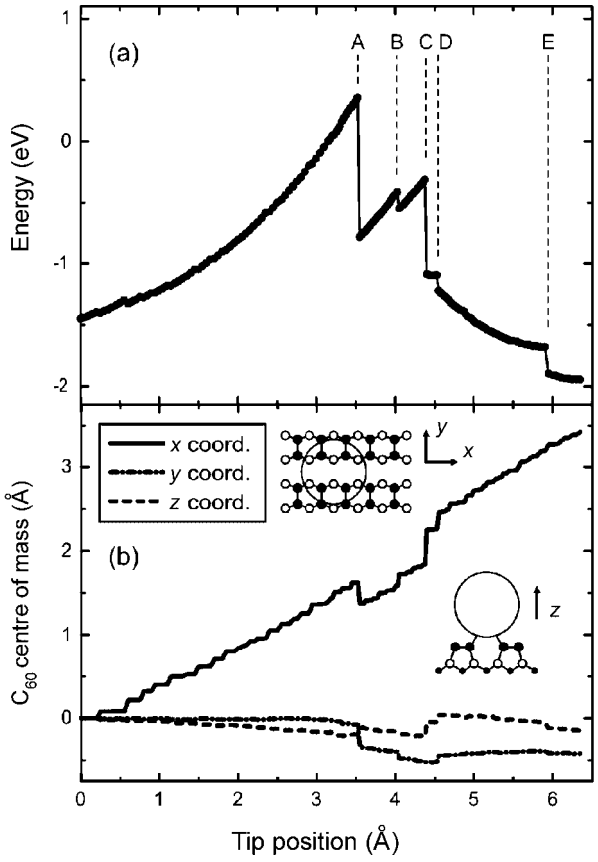


**Figure 2.** a) Calculated energy during the simulated manipulation of $C_{60}$ along the trough (*x* axis) through one lattice constant using the dangling-bond-terminated tip. Labels A–E correspond to bond-rearrangement events (see text and Figure 3). b) Coordinates (defined in the inset) of the center of mass of the $C_{60}$ molecule as a function of tip position.

position (Figure 2b). The chemical processes at these points have been analyzed using electron-density difference plots (see Figure 3) and found to correspond to different bond-rearrangement events: A) Following the initial rise in energy due to the repulsive tip–molecule interaction that results in a compression of $C_{60}$ (note the reduction by ca. 0.2 Å of the *z* coordinate), a bond is formed between $C_{60}$ and the tip. The energy reduction is accompanied by a reduction in the *x* coordinate (i.e., the molecule relaxes back towards the tip in forming the bond), and an increase in the *z* coordinate. Overall the system has lowered energy by reducing the molecular deformation and forming new covalent bonds. B) A reduction in energy occurs because of the formation of one of the new front $C_{60}$–Si surface bonds, followed by (C), the breaking of the rear $C_{60}$–surface bonds. D) A $C_{60}$–tip bond rearrangement occurs, and finally, E) the second front $C_{60}$–surface bond is formed, stabilizing the molecule in a different orientation (*t4g*, see Refs. [17,27]) at a neighboring lattice site.

We stress that once the tip–molecule bonds are formed, the tip continues to push the $C_{60}$ molecule and maintains a constant chemical contact with the molecule. There is an interval B–C during which the molecule pivots over two Si–C bonds, while the rear two Si–C bonds still exist and one new Si–C bond has already been formed. There is then a long interval (C–E) after which the two back bonds are severed when there are only three $C_{60}$–surface Si–C bonds, before the fourth bond is formed at point E. There are no large changes in molecular position accompanying the changes in energy due to re-bonding. The largest molecular displacement along the manipulation direction, approximately 0.35 Å, occurs at C when the back bonds break and should be compared with hops close to 2 Å, which are calculated in the absence of the tip.[17]

Our calculations confirm that the quasi-continuous displacement of the molecule is caused by the tip–$C_{60}$ bonding, which prevents the molecule from moving abruptly from the pivoting point into the next stable adsorption configuration; the tip stabilizes otherwise unfavorable configurations of the $C_{60}$ along

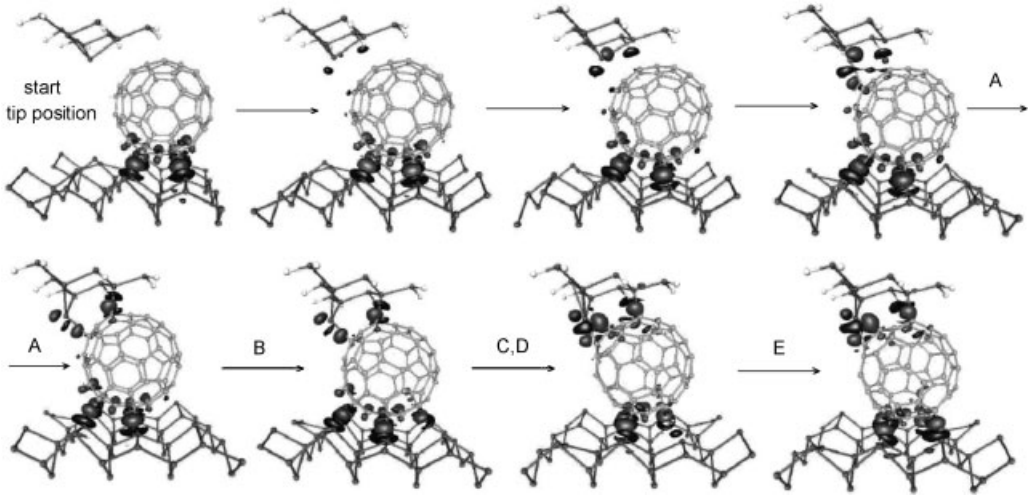


**Figure 3.** Electron-density difference plots for pushing the $C_{60}$ molecule with a dangling-bond-terminated tip. Black denotes the lack of, and dark gray the excess of electron density in the combined system (isosurfaces at $\pm 0.035$ *e*) compared to the isolated components. Steps A–E correspond to the bond-rearrangement events marked on the energy curve in Figure 2.

  

a constrained manipulation path. Nevertheless, the basic pivoting mechanism of the $C_{60}$ manipulation across the Si(001) surface is confirmed: the molecule rolls by breaking rear, and forming new front, C–Si bonds between the molecule and the surface. The sequence of the adsorption sites, $t4c \rightarrow t4g$, is also unchanged compared to the tip-free case and to our analytical prediction.[17]

We also comment on the range of tip positions for which the energy in Figure 2a is positive. For a simple system this would normally be interpreted as being due to an unphysical non-bonding state. However, for the complex three-body arrangement under discussion here, this represents an acceptable physical result: the displacement of the tip has adiabatically maneuvered the molecule into a metastable state. At each point along the manipulation path, the system is in a local energy minimum separated by a barrier from the global minimum, corresponding to the next stable $C_{60}$–surface configuration.

Similar calculations have been undertaken for a number of different model tips. In particular we have considered a tip with a similar geometry but with the apex atom passivated by a H atom. In addition, we have considered tips with a similar geometry that are rotated about the $z$ axis so that a different nanofacet impinges on the molecule. In all cases we observe similar behavior, in which constrained molecular rolling occurs and is stabilized by the formation of tip–molecule bonds. The stabilization of the molecule by the tip is also observed in our simulations of the $C_{60}$ manipulation perpendicular to the dimer rows: the molecule is clearly stabilized above the row because of the attractive interaction with the tip.

Although our constant-height manipulation simulations cannot be directly compared with our constant-current STM experiments, the discussed tip–molecule bond formation and elongated pivoting should be common features of both the manipulation modes, providing strong support for our model. In particular, we may assert that transition points in the line scan curves (e.g., A and B in Figure 1a) should correspond to rebonding events during the manipulation and translation of the molecule. Note that at finite temperatures, rebonding events may be smoothed out by thermal motion of atoms in the junction. This may explain why we do not observe additional features in our experimental tip trajectories within any elementary translation steps.

Accordingly we conclude that the finite-gradient traces observed in our data correspond to a constrained form of molecular manipulation. The tip–molecule–surface three-body interaction considered here leads to the stabilization of completely new molecular adsorption states. A requirement for these new states to exist is the formation of strong competing bonds between the molecule and both the surface and the tip. Since STM tips are commonly contaminated with the surface atoms, a strong molecule–surface interaction may generally be expected to lead to this type of behavior. Therefore, although our conclusions are based on the study of a single model system, we argue that they can be generally applied to any molecules that are strongly attached to a surface. Our results show clearly that under such conditions adsorbates, which are trapped in such a junction, may adopt bonding states and conformations that are not observed for a molecule on an isolated surface and may thus be considered as new adsorption states. It is hoped that these observations will stimulate further studies of bonding in this three-body system including, for example, control of adsorption geometries and hysteretic effects associated with reversing the tip direction following the formation of tip–molecule bonds. Finally we point out that, while our work is of central importance in understanding and interpreting the microscopic processes that occur during molecular manipulation experiments, it also has a much wider relevance to the studies of tribology at the atomic/molecular scale.[29–32]

## Experimental Section

Experiments were performed under ultrahigh vacuum (UHV) conditions using a p-type Si sample (B-doped, 1–10 Ω cm resistivity), which was prepared by outgassing (600 °C overnight) and annealing (1150 °C for 1–2 min) in order to form the $2 \times 1$ reconstruction. Sub-monolayers of $C_{60}$ were then deposited by sublimation from a Knudsen cell at a typical rate of 2–3 monolayers per hour. Images of the surface were acquired using an STM instrument (head provided commercially by WA Technology; electronics constructed in-house[33]) housed within the UHV system. STM images were acquired in constant-current mode (typical scanning parameters: −3 V sample voltage, 0.1 nA tunnel current) at room temperature. Electrochemically etched tungsten tips, which were cleaned by electron-beam heating, were used for both imaging and manipulation.

In each case, manipulation was achieved by first reducing the sample voltage and increasing the tunnel current (to typical values of −1 V and 1 nA, respectively) in order to extend the tip towards the surface. The tip was then moved across the surface in lateral steps of 0.14 Å towards a target molecule. After each lateral step, the tip height was adjusted to maintain constant current using a digital feedback loop. The tip height was recorded as the tip moved along this trajectory and a long dwell time (101 clock cycles at a frequency of 40 kHz) at each point was chosen so that the measured linescan corresponded to a sequence of quasistatic equilibrium positions.

We used the DFT SIESTA code,[34] which implements the Perdew–Burke–Ernzerhof (PBE) density functional[35] within the generalized gradient approximation (GGA), norm-conserving pseudo potentials, localized double-zeta polarized (DZP) basis sets, and periodic boundary conditions (see Ref. [17]). Electron density difference plots were obtained by subtracting the electron densities of the isolated surface, tip, and the molecule *in the geometry of the combined system* from the electron density of the latter.

**Keywords:**
density functional calculations · fullerenes · molecular adsorption · nanomanipulation · STM

[1] D. M. Eigler, E. K. Schweizer, *Nature* **1990**, *344*, 524.
[2] L. Bartels, G. Meyer, K.-H. Rieder, *Phys. Rev. Lett.* **1997**, *79*, 697.
[3] F. Moresco, G. Meyer, K.-H. Rieder, H. Tang, A. Gourdon, C. Joachim, *Phys. Rev. Lett.* **2001**, *87*, 088 302.

  

[4] F. Rosei, M. Schunack, P. Jiang, A. Gourdon, E. Laegsgaard, I. Stensgaard, C. Joachim, F. Besenbacher, *Science* **2002**, *296*, 328.
[5] P. H. Beton, A. W. Dunn, P. Moriarty, *Appl. Phys. Lett.* **1995**, *67*, 1075.
[6] T. A. Jung, R. R. Schlitter, J. K. Gimzewski, H. Tang, C. Joachim, *Science* **1996**, *271*, 181.
[7] L. Grill, K.-H. Rieder, F. Moresco, G. Rapenne, S. Stojkovic, X. Bouju, C. Joachim, *Nat. Nanotechnol.* **2007**, *2*, 95.
[8] F. Schreiber, *Prog. Surf. Sci.* **2000**, *65*, 151.
[9] F. Rosei, M. Schunack, Y. Naitoh, P. Jiang, A. Gourdon, E. Laegsgaard, I. Stensgaard, C. Joachim, F. Besenbacher, *Prog. Surf. Sci.* **2003**, *71*, 95.
[10] J. V. Barth, G. Costantini, K. Kern, *Nature* **2005**, *437*, 671.
[11] R. Otero, F. Rosei, F. Besenbacher, *Annu. Rev. Phys. Chem.* **2006**, *57*, 497.
[12] J. V. Barth, *Annu. Rev. Phys. Chem.* **2007**, *58*, 375.
[13] P. Moriarty, Y.-R. Ma, M. D. Upward, P. H. Beton, *Surf. Sci.* **1998**, *407*, 27.
[14] D. L. Keeling, M. J. Humphry, P. Moriarty, P. H. Beton, *Chem. Phys. Lett.* **2002**, *366*, 300.
[15] M. Kageshima, H. Ogiso, H. Tokumoto, *Surf. Sci.* **2002**, *517*, L557.
[16] D. L. Keeling, M. J. Humphry, R. H. J. Fawcett, P. H. Beton, C. Hobbs, L. Kantorovich, *Phys. Rev. Lett.* **2005**, *94*, 146 104.
[17] N. Martsinovich, C. Hobbs, L. Kantorovich, R. H. J. Fawcett, M. J. Humphry, D. L. Keeling, P. H. Beton, *Phys. Rev. B* **2006**, *74*, 085 304.
[18] R. M. Tromp, R. J. Hamers, J. E. Demuth, *Phys. Rev. Lett.* **1985**, *55*, 1303.
[19] X.-D. Wang, T. Hashizume, H. Shinohara, Y. Saito, Y. Nishina, T. Sakurai, *Phys. Rev. B* **1993**, *47*, 15923.
[20] D. Chen, D. Sarid, *Surf. Sci.* **1994**, *318*, 74.
[21] J. Weckesser, J. V. Barth, K. Kern, *Phys. Rev. B* **2001**, *64*, R161 404.
[22] Y. Shirai, A. J. Osgood, Y. Zhao, Y. Yao, L. Saudan, H. Yang, C. Yu-Hung, L. B. Alemany, T. Sasaki, J.-F. Morin, J. M. Guerrero, K. F. Kelly, J. M. Tour, *J. Am. Chem. Soc.* **2006**, *128*, 4854.
[23] R. Perez, M. C. Payne, I. Stich, K. Terakura, *Phys. Rev. Lett.* **1997**, *78*, 678.
[24] W. Hofer, A. S. Foster, A. L. Shluger, *Rev. Mod. Phys.* **2003**, *75*, 1287.
[25] Ó. Paz, I. Brihuega, J. M. Gómez-Rodríguez, J. M. Soler, *Phys. Rev. Lett.* **2005**, *94*, 056 103.
[26] C. Hobbs, L. Kantorovich, *Surf. Sci.* **2006**, *600*, 551.
[27] C. Hobbs, L. Kantorovich, J. Gale, *Surf. Sci.* **2005**, *591*, 45.
[28] S. Boys, F. Bernardi, *Mol. Phys.* **1970**, *19*, 553.
[29] *Fundamentals of Friction, Wear on the Nanoscale* (Eds: E. Gnecco, E. Meyer), Springer, Berlin **2007**.
[30] A. Socoliuc, R. Bennewitz, E. Gnecco, E. Meyer, *Phys. Rev. Lett.* **2004**, *92*, 14 301.
[31] K. Miura, S. Kamiya, N. Sasaki, *Phys. Rev. Lett.* **2003**, *90*, 055 509.
[32] O. M. Braun, *Phys. Rev. Lett.* **2005**, *95*, 126 104.
[33] M. J. Humphry, R. Chettle, P. J. Moriarty, M. D. Upward, P. H. Beton, *Rev. Sci. Instr.* **2000**, *71*, 1698.
[34] J. M. Soler, E. Artacho, J. D. Gale, A. García, J. Junquera, P. Ordejón, D. Sánchez-Portal, *J. Phys.: Condens. Matter* **2002**, *14*, 2745.
[35] J. Perdew, K. Burke, M. Ernzerhof, *Phys. Rev. Lett.* **1996**, *77*, 3865.

Received: July 24, 2007
Revised: December 2, 2007
Published online: May 26, 2008

  